

J. Serb. Chem. Soc. 87 (0) 1–15 (2022)
JSCS–11692

Powdered adsorbent obtained from bathurst burr biomass for methylene blue removal from aqueous solutions

GIANNIN MOSOARCA¹, COSMIN VANCEA^{1*}, SIMONA POPA^{1**},
MARIA ELENA RADULESCU-GRAD² AND SORINA BORAN¹

¹Politehnica University Timisoara, Faculty of Industrial Chemistry and Environmental Engineering, Bd. V. Parvan, No. 6, 300223, Timisoara, Romania and ²“Coriolan Dragulescu” Institute of Chemistry, Romanian Academy, Mihai Viteazu Bd. No. 24, 300223 Timisoara, Romania

(Received 16 March, revised 30 April, accepted 4 May 2022)

Abstract: Powdered adsorbent obtained from bathurst burr biomass was tested for methylene blue removal from aqueous solutions. SEM and FTIR analyses were used to characterize the adsorbent before and after adsorption. The influence of contact time, adsorbent dose, pH, initial dye concentration, ionic strength and temperature on the process were investigated. Kinetic, equilibrium and thermodynamic studies were conducted to analyse the process. The Taguchi method was used to establish the most suitable conditions for the dye adsorption. The process is spontaneous, favourable, and exothermic and the Freundlich isotherm and pseudo-second order kinetic model best describe it. The Taguchi method indicate that the ionic strength is the factor with the greatest influence on the adsorption process.

Keywords: low-cost adsorbent; dye adsorption; kinetic; equilibrium; thermodynamic; Taguchi method.

INTRODUCTION

Methylene blue is a thiazine cationic dye used in various fields and activities. It is widely used in the textile industry for dyeing cotton, wood, and silk due to its ease of application, good material resistance and economic benefits. In medicine it is used to treat methemoglobinemia, cyanide poisoning and urinary tract infections. It is also used as a colouring agent in diagnostic examination and surgery. Even if not strongly hazardous, the methylene blue can have negative effects on humans causing eye irritation, breathing difficulty, nausea, heart-beat increase, vomiting, diarrhea and jaundice. To avoid harmful impacts on aquatic

*,** Corresponding authors. E-mail: (*)cosmin.vancea@upt.ro; (**simona.popa@upt.ro
<https://doi.org/10.2298/JSC220316039M>

life and human health, the dye should be removed from wastewater before their discharging into natural effluents.¹⁻⁵

Scientific literature mentions many physicochemical and biological methods designed to remove the methylene blue dye from aqueous solutions: adsorption, coagulation, flocculation, ion exchange, precipitation, oxidation, chemical precipitation, electrochemical processes, photocatalytic processes, membrane processes and biodegradation. Very often, adsorption is the chosen process for dye retention due to its many advantages such as: simplicity, high efficiency, flexibility and low costs. An important number of adsorbents are known, among which an important role is played by natural materials that are cheap and available in large quantities.¹⁻¹⁰

Bathurst Burr (*Xanthium spinosum*) is a very invasive plant widespread in Europe, North America, Asia, Australia and partly in Africa. It has a very high resistance to drought, pollution and, in general, to any aggressive environmental conditions. It grows up to one meter tall and has a branched stem full of thorns. It can be found in lowland, hilly and low mountain areas, on pastures, abandoned land and roadsides. Due to its anti-inflammatory, disinfectant, diuretic, antidiabetic and antitumor properties, is used in traditional medicine.^{11,12}

The purpose of this study was to use the bathurst burr powder to remove the methylene blue dye from aqueous solutions by adsorption. The effect of contact time, adsorbent dose, pH, initial dye concentration, ionic strength and temperature on the adsorption process were monitored. Kinetic, equilibrium and thermodynamic studies were used to analyse the process. In order to establish the most suitable conditions for the dye adsorption, the process was optimized by the Taguchi method.

EXPERIMENTAL

The adsorbent material was obtained from the aerial part of bathurst burr mature plants, which were purchased from StefMar SRL, a local company that process and pack medicinal and aromatic plants. The adsorbent powder obtaining process was described elsewhere.¹³ The characteristics of adsorbent material, before and after adsorption, were examined by SEM analysis (Quanta FEG 250 scanning electron microscope at 1600× magnitude) and FTIR spectroscopy (Shimadzu Prestige-21 FTIR spectrophotometer). The point of zero charge (pH_{PZC}) was determined using the solid addition method.³

In the adsorption studies the influence of pH, adsorbent dose, dye concentration, time, temperature, and ionic strength was studied. Three independent replicates were performed for each test. During the experiments a constant mixing intensity was maintained. The pH was adjusted using NaOH and HCl solutions (0.1 M). NaCl as background electrolyte was used to study the effect of ionic strength. The methylene blue concentration was determined using a UV-Vis spectrophotometer at 664 nm wavelength.

The equilibrium and kinetics studies were assessed using the nonlinear equations of the Langmuir, Freundlich and Temkin isotherms and also, the nonlinear equations of the pseudo first-order, pseudo second-order and Elovich kinetic models.¹⁴⁻¹⁷ Each of these isotherm and kinetic models were evaluated through the statistical parameters determination coefficient

(R^2), sum of square error (SSE), chi-square (χ^2) and average relative error (ARE).¹⁷ The higher value for R^2 and the lower value for SSE , χ^2 and ARE were used as the criterion for determining the most suitable model.

The Taguchi method was used to optimize the dye removal experimental conditions. The L27 orthogonal array experimental design was employed to establish the influence of six controllable factors on methylene blue removal. Table I shows these factors and their levels. The Taguchi method evaluates the experimental results by signal-to-noise (S/N) ratio, defining the measurement of the response deviation from the desired value.¹⁸⁻²⁰ "The larger the better" option was used to maximize the S/N ratio and implicitly the highest dye removal efficiency. All calculations were performed with the Minitab 19 Software.

TABLE I. Controllable factors and their levels

Factor	Level 1	Level 2	Level 3
Time, min	1	10	30
Adsorbent dose, mg L ⁻¹	0.5	1.5	3.0
pH	2	6	10
Initial dye concentration, mg L ⁻¹	50	150	250
Ionic strength, mol L ⁻¹	0	0.1	0.2
Temperature, K	284	291	315

RESULTS AND DISCUSSION

Adsorbent surface characterization

Fig. 1 shows the SEM images of the adsorbent material surface at 3000 \times magnification. Before adsorption, the adsorbent surface has a porous aspect, suitable for dye adsorption (Fig. 1A).

After adsorption, the surface morphology has changed (Fig. 1B), indicating that pores, voids, or irregularities might be filled with the dye molecules.

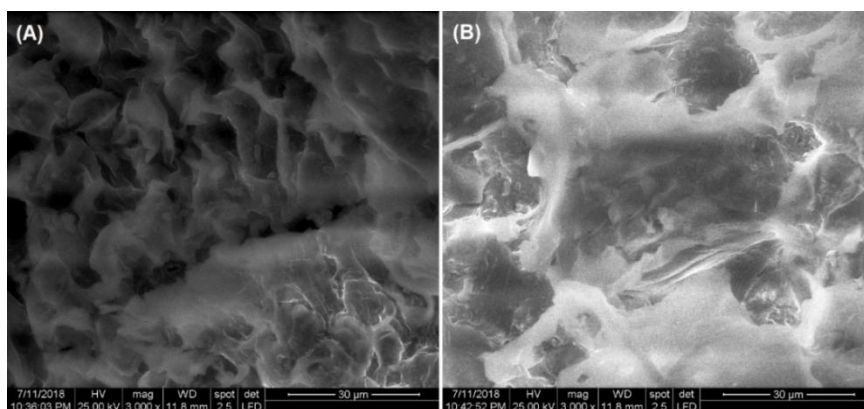


Fig. 1. SEM images of adsorbent surface: A) before and B) after adsorption.

The FTIR spectrum of adsorbent, depicted in Fig. 2, indicates that main components of bathurst burr powder are cellulose, hemicellulose, and lignin. The

identified peaks of the functional groups characteristic of these components are: 3448 cm^{-1} corresponds to O–H stretching of cellulose, Senthamaraikannan *et al.*²¹ found this peak in the spectra of natural cellulosic fibre from bark of *Albizia amara*; 2340 and 1630 cm^{-1} indicate O–H bending of adsorbed water, Tsuboi²² identifying both peaks in FTIR spectra of cellulose extracted from natural flax, ramie and cotton fibres and Karimi *et al.*²³ found the second peak in cellulose spectrum isolated from kenaf fibres; 2053 cm^{-1} – can be assigned to NCO from isocyanate groups, presence of this functional group being reported Salim *et al.*²⁴ in the lignin spectra extracted from bark of *Leucaena leucocephala*; 1368 cm^{-1} corresponds to C–H bending vibration in cellulose and hemicellulose, Labbe *et al.*²⁵ and Kubovský *et al.*²⁶ found this peak in spectra of aspen tree bark and oak wood respectively; 1000 cm^{-1} indicate C–O stretching, Liang and Marchesault²⁷ identifying this peak in in FTIR spectra of native cellulose; 542 cm^{-1} can be attributed to C–H bend, Salim *et al.*²⁴ found this band in the spectra of lignin extracted from native *Leucaena leucocephala* bark.

After absorption, the FTIR spectrum does not show significant differences compared to the one recorded before adsorption, which indicates that physical interactions are implied in the adsorption process.^{8,13}

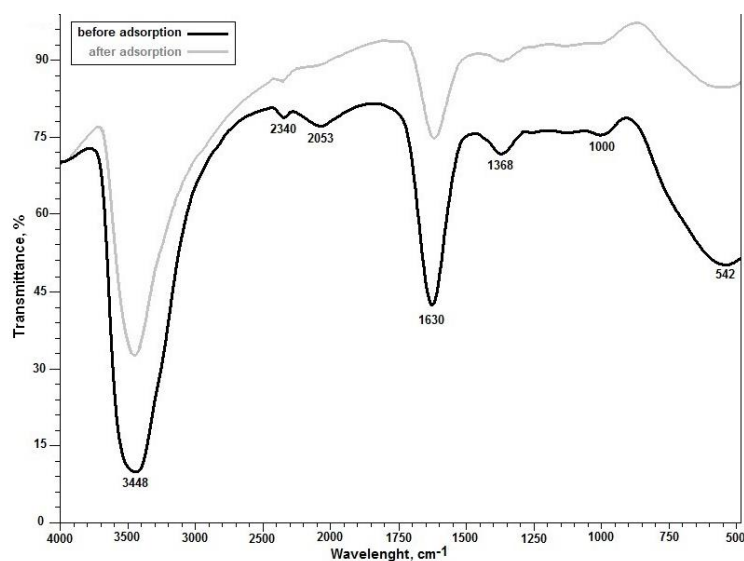


Fig. 2. FTIR spectra of adsorbent before and after dye adsorption.

The point of zero charge provides information on how an adsorbate will be adsorbed by an adsorbent material depending on the surface electrical charge.

If the solution pH is higher than pH_{PZC} , the adsorbent surface is negatively charged while a solution pH lower than pH_{PZC} leads to a positively charged ads-

orbent surface. Therefore, the adsorption of methylene blue will be favoured when the pH of the solution is higher than pH_{PZC} . The value of this parameter, determined using solid addition method, was 6.64 (Fig. 3).

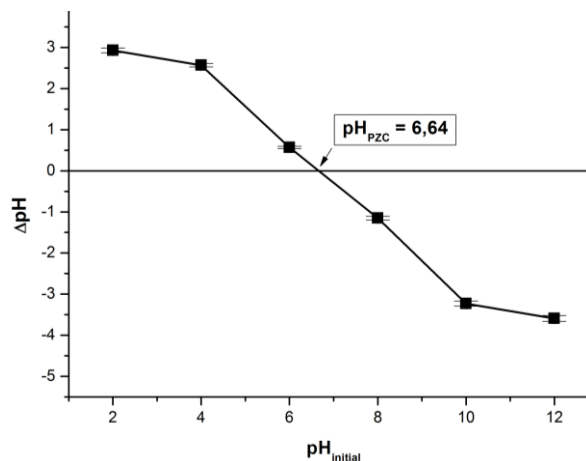


Fig. 3. Determination of point of zero charge (pH_{PZC}) based on the solid addition method.

The influence of contact time on adsorption process

In the first few minutes, the adsorption process is fast (Fig. 4) because many active adsorption sites are available on the surface of the material.^{6,7,10} As time goes on, these sites gradually take over and the adsorption capacity increases more slowly. After 30 min the equilibrium is reached, indicating that all the surface of the adsorbent is covered by dye molecules.^{6,7}

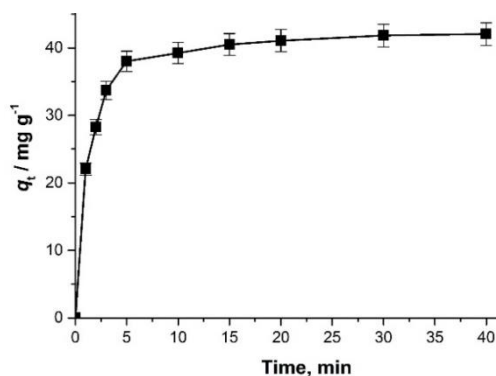


Fig. 4. Influence of contact time on adsorption capacity.

The equilibrium times obtained for similar adsorbents used for methylene blue removal from water were: 30 min for *Arthrospira platensis* biomass,²⁸ 50 min for *Haloxylon recurvum* stem biomass,²⁹ 60 min for *Euchema Spinosum* alga biomass³⁰ and 90 min for *Phragmites australis* biomass.³¹

The influence of adsorbent dose on adsorption process

The adsorbent dose influence upon the adsorption capacity together with the methylene blue removal efficiency are presented in Fig. 5. The two parameters behave differently as the adsorbent dose increases: the adsorption capacity decreases while the dye removal efficiency increases. At high adsorbent amounts the aggregation of particles can occur, and a large part of the active sites remains unsaturated. These two phenomena lead to a decrease of the adsorption capacity.^{7,9,10} The positive effect of a larger adsorbent quantity upon the removal efficiency is based on an increase of the surface area and thus of the number of sites available for adsorption.^{3,7,9} Similar observations have been reported in other studies on the methylene blue adsorption on other low-cost plant materials. When *Salix babylonica* leaves were used as adsorbent, an increase in adsorbent material dose from 0.2 to 15 g L⁻¹ led to an increase in dye removal efficiency of 36.88 % and a decrease in adsorption capacity of 98 %.⁷ In the case of citrus limetta peel use, it was observed that for an increase of the adsorbent dose from 0.4 to 2.0 g L⁻¹, removal efficiency increased rapidly by about 3 % while the adsorption capacity decreased by 91 %.¹⁰

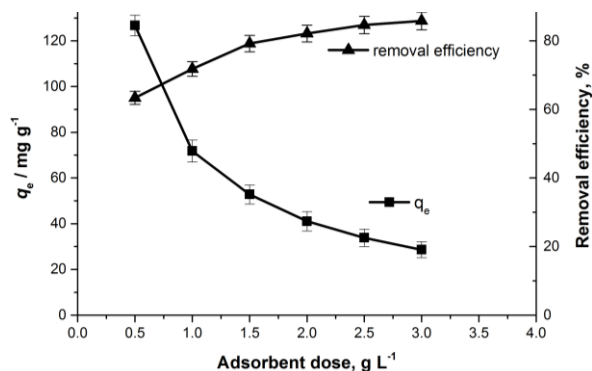


Fig. 5. Influence of adsorbent dose on adsorption capacity and removal efficiency.

The influence of pH on adsorption process

The effect of solution pH on adsorption capacity is depicted in Fig. 6. Increasing the value of this parameter has a positive effect on the adsorption capacity. The best results were obtained at a pH higher than 8. At these pH values, higher than the pH corresponding to the point of zero charge (pH_{PZC} 6.64), the adsorbent material surface is negatively charged, favouring the electrostatic attraction with the dye cations.^{3,10,32} Similar results were reported in other previous articles published in scientific literature. At pH > 8, increased adsorption capacities were recorded for adsorbent materials such as: *Salix babylonica* leaves,⁷ citrus limetta peel,¹⁰ *Phragmites australis* biomass³¹ and phoenix tree's leaves.³³

The relatively constant value of adsorption capacity at high pH indicates that in addition to the electrostatic attraction, other mechanisms are also involved in the adsorption process.³²

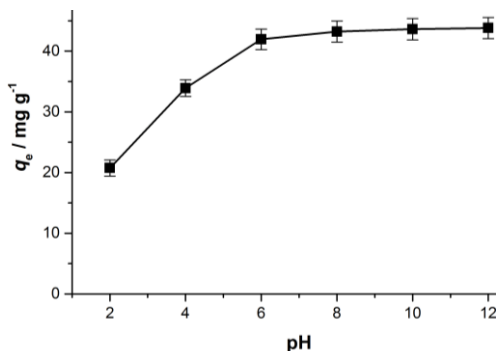


Fig. 6. Influence of pH on adsorption capacity.

The influence of initial dye concentration on adsorption process

The adsorption capacity and the dye removal efficiency values at different initial dye concentrations are shown in Fig. 7. The adsorption capacity increases while the dye removal efficiency decreases as the initial dye concentration increases. The first parameter behaviour is caused by the increase of the driving force resulting from the concentration gradient.^{32,33} The values of the second parameter decrease due to the accumulation of methylene blue molecules on the surface of the adsorbent which leads to saturation of the adsorption sites.^{6,28} Similar behaviours have been mentioned previously in other adsorption studies. Our study shows that an increase of the initial dye concentration from 50 to 200 mg L^{-1} leads to an increase of the adsorption capacity from 21.7 to 83.5 mg g^{-1} and a decrease of dye removal efficiency from 87.18 to 83.19 % respectively. For the same initial dye concentration variation range, other researchers reported an

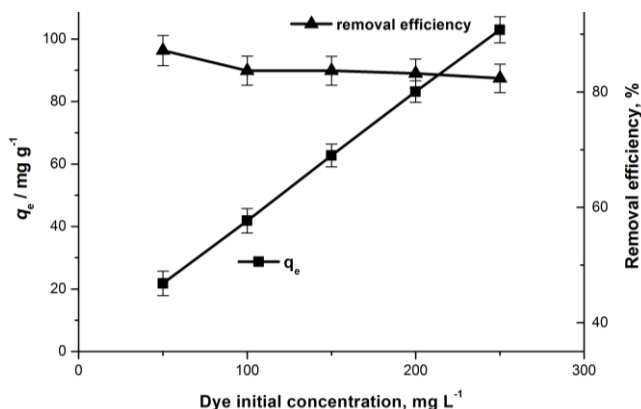


Fig. 7. Influence of dye initial concentration on adsorption capacity and removal efficiency.

increase in adsorption capacity from about 24 to 80 mg g⁻¹ and a decrease dye removal efficiency from 96 to 92 % when using weeping willow leaves⁷ as an adsorbent. Another study using *A. platensis* biomass²⁸ as adsorbent, an increase of the initial dye concentration from 6.25 to 100 mg L⁻¹ generates an increase of the adsorption capacity from 8 to 90 mg g⁻¹ and a dye removal efficiency decrease from 60 to about 45 %.

The influence of ionic strength on adsorption process

Increasing the solution ionic strength generates a decrease of the adsorption capacity, illustrated in Fig. 8, due to competition between methylene blue cations and sodium ions to occupy the available adsorption sites on the surface of the adsorbent.^{32,33} The unfavourable effect of ionic strength on methylene blue adsorption process was also mentioned in other studies. Thus, for *A. platensis* biomass,²⁸ lotus leaves³² and phoenix tree leaves³³ adsorbents an increase in ionic strength from 0 to 0.2 mol L⁻¹ leads to an adsorption capacity decrease of 72, 22 and 7 %, respectively.

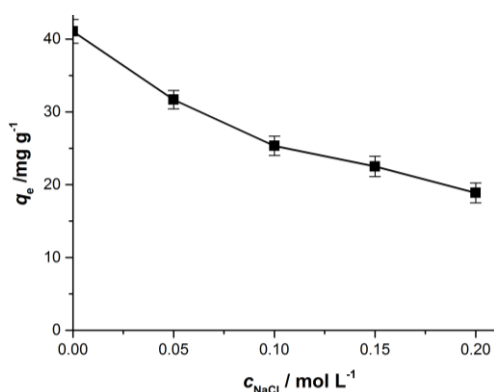


Fig. 8. Influence of ionic strength on adsorption capacity.

The influence of temperature on adsorption process

According to Fig. 9 the adsorption capacity decreases with increasing the temperature indicating that the process is exothermic in nature. The binding forces between the adsorbent surface and the adsorbate molecules become weaker with increasing temperature.^{34,35} Similar observations have been reported by others previous articles. When *Salix babylonica* leaves,⁷ *Haloxylon recurvum* plant stems²⁹ and Natural Muscovite Clay³⁴ were used as adsorbent materials to remove methylene blue from aqueous solutions, a negative effect of temperature rise on the adsorption capacity was observed.

Equilibrium isotherms

In order to study the interactions between the dye molecules and the adsorbent surface three isotherms were tested: Langmuir, Freundlich and Temkin.

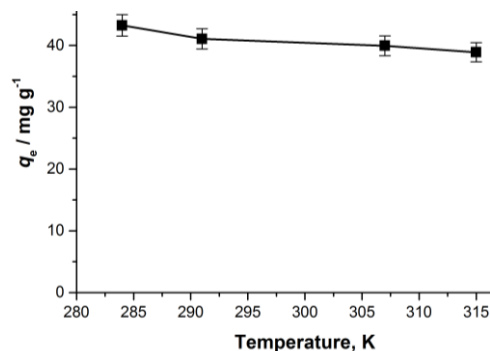


Fig. 9. Influence of temperature on adsorption capacity.

Fig. 10 shows the plots of the tested adsorption isotherms (non-linear forms). The values of adsorption isotherms constants and also, of the corresponding error functions (R^2 , SSE , χ^2 , ARE) are summarized in Table II.

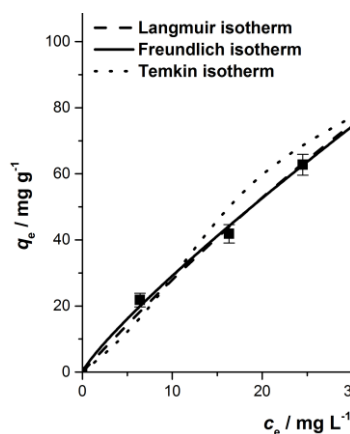


Fig. 10. The tested adsorption isotherms (non-linear forms) for the methylene blue adsorption.

Both the Langmuir isotherm and the Freundlich isotherm characterize very well the adsorption process (Fig. 10). Considering the higher value for determination coefficient (R^2) and the lower values of SSE , χ^2 and ARE it can be concluded that Freundlich isotherm best describes the process. The obtained results agree with those mentioned by other researchers in methylene blue adsorption studies, this isotherm characterizing the dye retention processes on adsorbent materials obtained from *Elaeis guineensis* leaves,⁴ *Haloxylon recurvum* stems²⁹ and *Euchema Spinosum* alga.³⁰

Table III shows a comparison between the maximum adsorption capacities values for methylene blue adsorption using similar low-cost adsorbents.

Adsorption kinetics

The kinetics of the methylene blue adsorption process on the studied adsorbent was investigated by means of kinetic models (non-linear forms): pseudo-

-first order, pseudo-second order and Elovich. The plots of these kinetic models and the value of their specific constants are illustrated in Fig. 11 and Table IV, respectively. The values of the coefficients of determination (R^2) for all models are above 0.96, the highest recorded value was for the pseudo-second order model while the lowest value corresponds to the Elovich model. The calculated values of the error functions (χ^2 , SSE and ARE) are the lowest for the pseudo-second order model.

TABLE II. Adsorption isotherms models constants and the corresponding error functions

Isotherm model	Parameter	Value
Langmuir non-linear	$K_L / \text{L mg}^{-1}$	0.006±0.001
	$q_{\text{max}} / \text{mg g}^{-1}$	485.1±9.23
	R^2	0.9978
	χ^2	0.78
	SSE	17.37
	$ARE / \%$	5.08
Freundlich non-linear	$K_f / \text{mg g}^{-1}$	4.07±0.74
	$1/n$	0.85±0.07
	R^2	0.9985
	χ^2	0.32
	SSE	10.90
	$ARE / \%$	3.39
Temkin non-linear	$K_T / \text{L mg}^{-1}$	0.220±0.043
	$B / \text{kJ g}^{-1}$	58.77±6.94
	R^2	0.9584
	χ^2	7.81
	SSE	307.29
	$ARE / \%$	18.81

TABLE III. The maximum adsorption capacities (mg g^{-1}) for methylene blue on different low-cost adsorbents

Adsorbent	Value
<i>Citrullus colocynthis</i> seeds ⁶	18.8
<i>Phragmites australis</i> biomass ³¹	22.7
<i>Haloxylon recurvum</i> stems ²⁹	22.9
<i>Salix babylonica</i> leaves ⁷	60.9
<i>Daucus carota</i> leaves ³	66.5
Phoenix tree leaves ³³	80.9
<i>Elaeis guineensis</i> leaves ⁴	103.0
Dry bean pods husks ⁸	121.1
Fava bean peel ¹	140.0
lotus leaf ³²	221.7
Citrus limetta peel ¹⁰	227.3
<i>Arthrospira platensis</i> biomass ²⁸	312.5
Bathurst burr biomass (this study)	485.1
<i>Euchema Spinosum</i> algae ³⁰	833.3

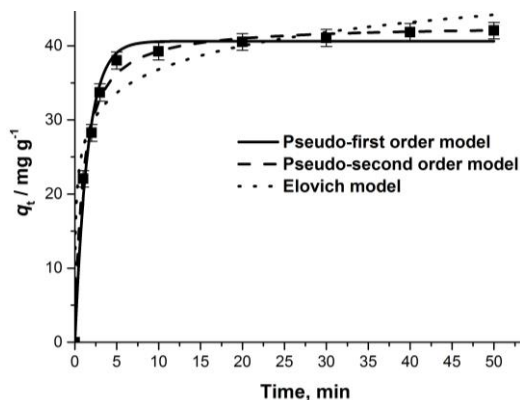


Fig. 11. The tested kinetic models (non-linear forms) for the methylene blue adsorption.

TABLE IV. Kinetic models constants and the corresponding error functions

Kinetic model	Parameter	Value
Pseudo-first order non-linear	k_1 / min^{-1}	0.648 ± 0.051
	$q_{e,\text{calc}} / \text{mg g}^{-1}$	40.63 ± 0.4
	R^2	0.9899
	χ^2	0.61
	SSE	16.37
	ARE / %	13.48
Pseudo-second order non-linear	k_2 / min^{-1}	0.025 ± 0.004
	$q_{e,\text{calc}} / \text{g mg}^{-1} \text{min}^{-1}$	42.86 ± 0.38
	R^2	0.9962
	χ^2	0.17
	SSE	5.84
	ARE / %	11.59
Elovich non-linear	$a / \text{g mg}^{-1}$	0.218 ± 0.048
	$b / \text{mg g}^{-1} \text{min}^{-1}$	1434 ± 124
	R^2	0.9635
	χ^2	1.95
	SSE	57.41
	ARE / %	15.84

These results indicate that the adsorption process is best described by this kinetic model. The conclusion is also supported by the calculated value of equilibrium adsorption capacity 42.86 mg g^{-1} which is very close to experimental value 42.05 mg g^{-1} . The pseudo-second order kinetic model also characterized other similar methylene blue adsorption processes on other adsorbents based on *Salix babylonica* leaves,⁷ corn cobs,⁹ *Euchema Spinosum* macro-alga,³⁰ *Phragmites australis* biomass³¹ and lotus leaves.³²

Thermodynamic parameters

The thermodynamic parameters of dye adsorption process, calculated bases on experimental results obtained at 284, 291, 307 and 315 K, are presented in

Table V. The negative values of standard Gibbs energy change (ΔG^0) and standard enthalpy change (ΔH^0) indicate a spontaneous, favourable and exothermic process. The positive value of standard entropy change (ΔS^0) shows an increase randomness at solid–liquid interface. The value of ΔG^0 is in the range -20 to 0 kJ mol $^{-1}$ and the ΔH^0 value is lower than 40 kJ mol $^{-1}$, therefore the main mechanism involved in absorption is physisorption.^{7,29,31,34,35}

TABLE V. Thermodynamic parameters for the methylene blue adsorption onto bathurst burr powder

$\Delta G^0 / \text{kJ mol}^{-1}$				$\Delta H^0 / \text{kJ mol}^{-1}$	$\Delta S^0 / \text{J mol}^{-1} \text{K}^{-1}$
284 K	291 K	307 K	315 K		
-19.04	-19.18	-19.78	-19.91	-1.26	3.60

Optimization adsorption parameters by Taguchi method

The L27 orthogonal array and the obtained results after each run, for dye removal efficiency and the S/N ratios, are summarized in Table VI. The order of the controllable factors' significance (Table VII) was established using the rank of S/N ratio and delta values (difference between the highest and lowest average response values for each factor).¹⁸

TABLE VI. Experimental layout of L27 orthogonal array

τ / min	Adsorbent dose, mg L $^{-1}$	pH	Initial dye concentration, mg L $^{-1}$	Ionic strength mol L $^{-1}$	T / K	Removal efficiency, %	S/N
1	0.5	2	50	0.0	284	18.73	25.45
1	0.5	2	50	0.1	291	10.97	20.80
1	0.5	2	50	0.2	315	7.74	17.78
1	1.5	6	250	0.1	284	40.27	32.09
1	1.5	6	250	0.2	291	23.59	27.45
1	1.5	6	250	0.0	315	16.64	24.42
1	3.0	10	150	0.2	284	44.93	33.05
1	3.0	10	150	0.0	291	26.32	28.40
1	3.0	10	150	0.1	315	18.57	25.37
10	0.5	10	250	0.2	284	27.61	28.82
10	0.5	10	250	0.0	291	19.52	25.81
10	0.5	10	250	0.1	315	40.25	32.09
10	1.5	2	150	0.0	284	56.74	35.07
10	1.5	2	150	0.1	291	40.12	32.06
10	1.5	2	150	0.2	315	82.71	38.35
10	3.0	6	50	0.1	284	42.06	32.47
10	3.0	6	50	0.2	291	29.74	29.46
10	3.0	6	50	0.0	315	61.31	35.75
30	0.5	6	150	0.1	284	23.53	27.43
30	0.5	6	150	0.2	291	48.60	33.73
30	0.5	6	150	0.0	315	28.42	29.07
30	1.5	10	50	0.2	284	30.66	29.73

TABLE VI. Continued

τ / min	Adsorbent dose, mg L ⁻¹	pH	Initial dye concentration, mg L ⁻¹	Ionic strength mol L ⁻¹	T / K	Removal efficiency, %	S/N
30	1.5	10	50	0.0	291	63.32	36.03
30	1.5	10	50	0.1	315	37.02	31.37
30	3.0	2	250	0.0	284	42.43	32.55
30	3.0	2	250	0.1	291	87.64	38.85
30	3.0	2	250	0.2	315	51.25	34.19

TABLE VII. Response table for signal-to-noise ratios

Level	Time	Adsorbent dose	pH	Initial dye concentration	Ionic strength	Temperature
1	26.78	28.76	26.10	30.57	33.94	30.74
2	31.85	30.70	32.21	30.21	29.74	30.29
3	32.24	31.40	32.55	30.08	27.18	29.83
Delta	5.46	2.63	6.46	0.49	6.75	0.92
Rank	3	4	2	6	1	5

The factor having the highest influence on the adsorption process was the ionic strength while the factor with the least influence was initial dye concentration. Correlating the data from Table I and Table VI, the optimum adsorption conditions were: time 30 min, adsorbent dose 3 mg L⁻¹, pH 10, initial dye concentration 50 mg L⁻¹, no ions and temperature 284 K.

CONCLUSION

Powdered material obtained from bathurst burr biomass is an efficient low-cost and easily available adsorbent for methylene blue removal from aqueous solutions. The adsorption is influenced by contact time, adsorbent dose, pH, initial dye concentration, ionic strength and temperature and is best described by Freundlich isotherm and pseudo-second order kinetic model. The process is spontaneous, favourable and exothermic and the main mechanism involved is physisorption. The ionic strength is the factor with the highest influence on the process and initial dye concentration least influences the adsorption.

ИЗВОД

АДСОРБЕНТ У ПРАХУ ДОБИЈЕН ИЗ БИОМАСЕ *Xanthium spinosum* ЗА УКЛАЊАЊЕ МЕТИЛЕНСКОГ ПЛАВОГ ИЗ ВОДЕНИХ РАСТВОРА

GIANNIN MOSOARCA¹, COSMIN VANCEA¹, SIMONA POPA¹, MARIA ELENA RADULESCU-GRAD²
и SORINA BORAN¹

¹Politehnica University Timisoara, Faculty of Industrial Chemistry and Environmental Engineering, Bd. V. Parvan, No. 6, 300223, Timisoara, Romania и ²"Coriolan Dragulescu" Institute of Chemistry, Romanian Academy, Mihai Viteazu Bd. No. 24, 300223 Timisoara, Romania

Адсорбент у праху добијен из *Xanthium spinosum* биомасе је испитиван за уклањање метиленског плавог из водених раствора. SEM и FTIR анализе су коришћене за карактеризацију адсорбента пре и након адсорпције. Испитан је утицај времена контакта, дозе

адсорбента, рН, почетне концентрације боје, јонске јачине и температуре на процес адсорпције. Кинетичка, равнотежна и термодинамичка испитивања су вршена ради анализе процеса адсорпције. Тагучи метод је коришћен да би се одредили најбољи услови за адсорпцију боје. Процес је спонтан, фаворизован, егзотерман, описује га Фројндлихова изотерма и кинетички модел псеудо-другог реда. Тагучи метод указује да је јонска јачина фактор који има највећи утицај на процес адсорпције.

(Примљено 16. марта, ревидирано 30. априла, прихваћено 4. маја 2022)

REFERENCES

1. O. S. Bayomie, H. Kandeel, T. Shoeib, H. Yang, N. Youssef, M. M. H. El-Sayed, *Sci. Rep.* **10** (2020) 7824 (<https://doi.org/10.1038/s41598-020-64727-5>)
2. N. Choudhary, V. K. Yadav, K. K. Yadav, A. I. Almohana, S. F. Almojil, G. Gnanamoorthy, D. H. Kim, S. Islam, P. Kumar, B. H. Jeon, *Water* **13** (2021) 3206 (<https://doi.org/10.3390/w13223206>)
3. A. K. Kushwaha, N. Gupta, M. C. Chattopadhyaya, *J. Saudi. Chem. Soc.* **18** (2014) 200 (<https://doi.org/10.1016/j.jscs.2011.06.011>)
4. H. D. Setiabudi, R. Jusoh, S. F. R. M. Suhaimi, S. F. Masrur, *J. Taiwan Inst. Chem. Eng.* **63** (2016) 363 (<https://doi.org/10.1016/j.jtice.2016.03.035>)
5. K. Sharma, S. Sharma, V. Sharma, P. K. Mishra, A. Ekielski, V. Sharma, V. Kumar, *Nanomaterials* **11** (2021) 1403 (<https://doi.org/10.3390/nano11061403>)
6. W. M. Alghamdi, I. El Mannoubi, *Processes* **9** (2021) 1279 (<https://doi.org/10.3390/pr9081279>)
7. A. Khodabandehloo, A. Rahbar-Kelishami, H. Shayesteh, *J. Mol. Liq.* **244** (2017) 540 (<https://doi.org/10.1016/j.molliq.2017.08.108>)
8. G. Mosoarca, S. Popa, C. Vancea, S. Boran, *Materials* **14** (2021) 5673 (<https://doi.org/10.3390/ma14195673>)
9. P. M. K. Reddy, P. Verma, C. Subrahmanyam, *J. Taiwan Inst. Chem. Eng.* **58** (2016) 500 (<https://doi.org/10.1016/j.jtice.2015.07.006>)
10. S. Shakoor, A. J. Nasar, *Taiwan. Inst. Chem. Eng.* **66** (2016) 154 (<https://doi.org/10.1016/j.jtice.2016.06.009>)
11. L. R. G. Holm, D. L. Plucknett, J. V. Pancho, J. P. Herberger, *The world's worst weeds. Distribution and biology*, University Press of Hawaii, Honolulu, HI, 1977 (ISBN 0824802950)
12. G. Raman, K. T. Park, J. H. Kim, S. J. Park, *BMC Genomics* **21** (2020) 855 (<https://doi.org/10.1186/s12864-020-07219-0>)
13. G. Mosoarca, C. Vancea, S. Popa, S. Boran, *Materials* **14** (2021) 5861 (<https://doi.org/10.3390/ma14195861>)
14. G. L. Dotto, N. P. G. Salau, J. S. Piccin, T. R. S. Cadaval, L. A. A. de Pinto, in *Adsorption Processes for Water Treatment and Purification*, A. Bonilla-Petriciolet, D. Mendoza-Castillo, H. Reynel-Ávila, Eds., Springer, Cham, 2017, p. 53 (https://doi.org/10.1007/978-3-319-58136-1_3)
15. V. M. Esquerdo, T. M. Quintana, G. L. Dotto, L. A. A. Pinto, *Reac. Kinet. Mech. Cat.* **116** (2015) 105 (<http://doi.org/10.1007/s11144-015-0893-5>)
16. M. S. Netto, J. Georgin, D. S. P. Franco, E. S. Mallmann, E. L. Foletto, M. Godinho, D. Pinto, G. L. Dotto, *Environ. Sci. Pollut. Res.* **29** (2022) 3672 (<https://doi-org.libproxy.viko.lt/10.1007/s11356-021-15366-4>)

17. J. S. Piccin, T. R. S. Cadaval, L. A. A. de Pinto, G. L. Dotto, in *Adsorption Processes for Water Treatment and Purification*, A. Bonilla-Petriciolet, D. Mendoza-Castillo, H. Reynel-Ávila, Eds., Springer, Cham, 2017, p. 19 (https://doi.org/10.1007/978-3-319-58136-1_2)
18. J. A. Fernandez-Lopez, J. M. Angosto, M. J. Roca, M. Doval Minarro, *Sci. Total Environ.* **653** (2019) 55 (<https://doi.org/10.1016/j.scitotenv.2018.10.343>)
19. S. R. Korake, P. D. Jadhao, *Heliyon* **6** (2020) e05755 (<https://doi.org/10.1016/j.heliyon.2020.e05755>)
20. S. S. Madan, K. L. Wasewar, *J. Appl. Res. Technol.* **15** (2017) 332 (<https://doi.org/10.1016/j.jart.2017.02.007>)
21. P. Senthamarakannan, M. R. Sanjay, K. S. Bhat, N. H. Padmaraj, M. Jawaid, *J. Nat. Fibers* **16** (2019) 1124 (<http://doi.org/10.1080/15440478.2018.1453432>)
22. Tsuboi L. M. F. Pardo, A. G. Córdoba, J. E. L. Galán, *DYNA* **86** (2019) 98 (<http://doi.org/10.15446/dyna.v86n210.75757>)
23. S. Karimi, P. M. Tahir, A. Karimi, A. Dufresne, A. Abdulkhani, *Carbohydr. Polym.* **101** (2013) 878 (<http://doi.org/10.1016/j.carbpol.2013.09.106>)
24. R. Md Salim, J. Asik, M. S. Sarjadi, *Wood Sci. Technol.* **55** (2021) 295 (<https://doi.org/10.1007/s00226-020-01258-2>)
25. N. Labbe, T. G. Rials, S. S. Kelley, Z. M. Cheng, J. Y. Kim, Y. Li, *Wood Sci. Technol.* **39** (2005) 61 (<https://doi.org/10.1007/s00226-004-0274-0>)
26. I. Kubovský, D. Kačíková, F. Kačík, *Polymers* **12** (2020) 485 (<https://doi.org/10.3390/polym12020485>)
27. C. Y. Liang, R. H. Marchessault, *J. Polym. Sci.* **39** (1959) 269 (<http://doi.org/10.1002/pol.1959.1203913521>)
28. D. Mitrogiannis, G. Markou, A. Çelekli, H. J. Bozkurt, *Environ. Chem. Eng.* **3** (2015) 670 (<http://doi.org/10.1016/j.jece.2015.02.008>)
29. W. Hassan, U. Farooq, M. Ahmad, M. Athar, M. A. Khan, *Arab. J. Chem.* **10** (2017) S1512 (<https://doi.org/10.1016/j.arabjc.2013.05.002>)
30. N. Mokhtar, E. A. Aziz, A. Aris, W. F. W. Ishak, N. S. M. Ali, *J. Environ. Chem. Eng.* **5** (2017) 5721–5731 (<https://doi.org/10.1016/j.jece.2017.10.043>)
31. G. B. Kankiliç, A. U. Metin, I. Tüzün, *Ecol. Eng.* **86** (2016) 85 (<https://doi.org/10.1016/j.ecoleng.2015.10.024>)
32. X. Han, W. Wang, X. Ma, *Chem. Eng. J.* **171** (2011) 1 (<http://doi.org/10.1016/j.cej.2011.02.067>)
33. R. Han, W. Zou, W. Yu, S. Cheng, Y. Wang, J. Shi, *J. Hazard. Mater.* **141** (2007) 156 (<https://doi.org/10.1016/j.jhazmat.2006.06.107>)
34. O. Amrhar, A. Berisha, L. El Gana, H. Nassali, M. S. Elyoubi, *Int. J. Environ. Anal. Chem.* (2021) (<https://doi.org/10.1080/03067319.2021.1897119>)
35. C. Saucier, M. A. Adebayo, E. C. Lima, L. D. T. Prola, P. S. Thue, C. S. Umpierrez, M. J. Puchana-Rosero, F. M. Machado, *Clean (Weinh)* **43** (2015) 1389 (<https://doi.org/10.1002/clen.201400669>).